DEM GENERATION FROM ASTER SATELLITE DATA

Iosif VOROVENCII, Assoc. Prof. PhD. Eng. Ec. - University "Transilvania" of Brasov, Romania, icatop@yahoo.com
Gheorghe CHITEA, Prof. PhD. Eng. - University "Transilvania" of Brasov, Romania, gchitea@unitbv.ro
Eugen IORDACHE, Assist. Lect. PhD. Eng.- University "Transilvania" of Brasov, Romania, i.eugen@unitbv.ro
Marius MIHAILA, Assist. Lect. PhD. Stud. - University "Transilvania" of Brasov, Romania, m.mihăilă@unitbv.ro

***Abstract**: Obtaining or creating a digital terrain model (DEM) for rough terrain is difficult in some areas while in others is very expensive. The ASTER sensor is an instrument on board of Terra (EO-1) launched in 1999 which has 14 spectral bands that cover the spectrum from visible to thermal infrared. Technically, ASTER consists of 3 subsystems: VNIR, SWIR and TIR. The VNIR subsystem is a pushbroom scanner that capture time in green, red and near infrared range with a spatial resolution of 15 meters in the nadir direction. In addition to the nadir-looking optics that is the second one, which point backwards and records in the infrared only. This constellation allows to generate digital elevation model from the VNIR band VNIR band 3nadir and 3backwards. This article discusses aspects regarding the way to obtain the DEM from ASTER satellite images, the steps involved and the resulting product quality.*

***Keywords**: DEM, ASTER images, 3nadir, 3backwards*

1. General aspects about ASTER

Terra is the first of a series of multi-instrument spacecraft forming NASA's Earth Observing System (EOS). EOS consists of a science component and a data information system (EOSDIS) supporting a coordinated series of polar-orbiting and low inclination satellites for long-term global observations of the land surface, biosphere, solid Earth, atmosphere, and oceans. By enabling improved understanding of the Earth as an integrated system, the EOS program has benefits for us all. In addition to ASTER, the other instruments on Terra are the Moderate-Resolution Imaging Spectroradiometer (MODIS), Multi-angle Imaging Spectro-Radiometer (MISR), Clouds and the Earth's Radiant Energy System (CERES), and Measurements of Pollution in the Troposphere (MOPITT). As the only high spatial resolution instrument on Terra, ASTER is the "zoom lens" for the other instruments, 30 minutes behind Landsat ETM+ (Abrams et al.). It was placed in a 705 km (at equator) sun synchronous orbit with descending node crossing at about 10:30 am local solar time and the orbital inclination of 98.2 degrees. The ASTER sensor will eventually image the entire Earth between latitude 80 north and 80 south.

The Advanced Spaceborne Thermal Emission and Reflection Radiometer (ASTER) is an advanced multispectral imager that was launched on board NASA's Terra spacecraft in December, 1999. ASTER covers a wide spectral region with 14 bands from the *visible* to the *thermal infrared* with high spatial, spectral and radiometric resolution. An additional backward-looking near-infrared band provides stereo coverage. The spatial resolution varies with wavelength: 15 m in the visible and near-infrared (VNIR), 30 m in the short wave infrared (SWIR), and 90 m in the thermal infrared (TIR). Each ASTER scene covers an area of 60 x 60 km (Abrams et al.).

ASTER can acquire data over the entire globe with an average duty cycle of 8% per orbit. This translates to acquisition of about 650 scenes per day, that are processed to Level-1A; of these, about 150 are processed to Level-1B. All 1A and 1B scenes are transferred to the EOSDIS archive at the EROS Data Center's (EDC) Land Processes Distributed Active Archive Center (LP-DAAC), for storage, distribution, and processing to higher-level data products. All ASTER data products are stored in a specific implementation of Hierarchical Data Format called HDF-EOS (Abrams et al.).

Another pronounced feature of ASTER is the capability to collect information, which leads to the production of stereoscopic data by combining them with high spatial resolution spectral information. ASTER band3 in VNIR (0.78 -0.86μm) can observe nadir-looking (3N) and backward looking (3B) data simultaneously. Stereoscopic data can be produced by the combination of these data. Also, based on the stereoscopic data, digital elevation model (DEM) can be processed. In this way, ASTER data can add three-dimensional information on topographic map.

The ASTER instrument has two types of Level-1 data: Level-1A and Level-1B data. Level-1A data are formally defined as reconstructed, unprocessed instrument data at full resolution. According to this definition, the ASTER Level-1A data consist of the image data, the radiometric coefficients, the geometric coefficients and other auxiliary data without applying the coefficients to the image data to maintain the original data values. The Level-1B data are generated applying these coefficients for radiometric calibration and geometric resampling. The ortho image is the image observed just above the target point. This means the ortho image includes no terrain error. The ortho image can be generated by correcting the terrain error using the elevation data for each pixel and the off-nadir observation angle. The 3D ortho product is the ortho product with the elevation data for each pixel, generated from the Level-1A data. Its formal name is Level-3A01. The instrument geometric parameters such as the line of sight (LOS) vectors and the pointing axis vectors were precisely adjusted through a validation process using numerous GCPs. The DEM data, which is processed using only these system parameters, has been demonstrated to have extremely good accuracy.

In 3D ortho data processing, the level-1A data is used as input image data. Moreover, the Level-A01X (DEM XYZ) data is used as geolocation information for providing ortho graphic projection and map coordinates projection features to the Level-1A data. After performing collection to the Level-1A data and the DEM data, a geometric conversion is performed on the image data. At that time, the SWIR parallax errors in the along-track direction due to the detector alignment and in the cross-track direction due to the Earth rotation are also corrected (Baipeng et al., 2008).

2. The ASTER Instrument

ASTER is a cooperative effort between NASA and Japan's Ministry of Economy Trade and Industry (METI) formerly known as Ministry of International Trade and Industry (MITI), with the collaboration of scientific and industry organizations in both countries. The ASTER instrument consists of three separate instrument subsystems: the Visible and Near-infrared (VNIR) has three bands with a spatial resolution of 15 m, and an additional backward telescope for stereo; the Shortwave Infrared (SWIR) has 6 bands with a spatial resolution of 30 m; and the Thermal Infrared (TIR) has 5 bands with a spatial resolution of 90 m. Each subsystem operates in a different spectral region, with its own telescope(s), and is built by a different Japanese company. In addition, one more telescope is used to view backward in the near-infrared spectral band (band 3B) for stereoscopic capability (Abrams et. al.).

The VNIR instrument subsystem consists of two independent telescope assemblies to minimize image distortion in the backward and nadir looking telescopes. The detectors for each of the bands consist of 5000 element silicon charge-coupled detectors (CCD's). Only 4000 of these detectors are used at any one time. A time lag occurs between the acquisition of the backward image and the nadir image. During this time earth rotation displaces the image center. The VNIR subsystem automatically extracts the correct 4000 pixels based on orbit position information supplied by the EOS platform (Abrams et. al.).

The VNIR optical system is a reflecting-refracting improved Schmidt design. The backward looking telescope focal plane contains only a single detector array and uses an interference filter for wavelength discrimination. The focal plane of the nadir telescope contains 3 line arrays and uses a dichroic prism and interference filters for spectral separation allowing all three bands to view the same area simultaneously. The telescope and detectors are maintained at 296 ± 3K using thermal control and cooling from a platform-provided cold plate. On-board calibration of the two VNIR telescopes is accomplished with either of two independent calibration devices for each telescope. The radiation source is a halogen lamp. A diverging beam from the lamp filament is input to the first optical element (Schmidt corrector) of the telescope subsystem filling part of the aperture. The detector elements are uniformly irradiated by this beam. In each calibration device, two silicon photo-diodes are used to monitor the radiance of the lamp. One photo-diode monitors the filament directly and the second monitors the calibration beam just in front of the first optical element of the telescope. The temperatures of the lamp base and the photo-diodes are also monitored. Provision for electrical calibration of the electronic components is also provided (Abrams et. al.).

The system signal-to-noise is controlled by specifying the NE delta rho (ρ) to be < 0.5% referenced to a diffuse target with a 70% albedo at the equator during equinox. The absolute radiometric accuracy is ± 4% or better.

The VNIR subsystem produces by far the highest data rate of the three ASTER imaging subsystems. With all four bands operating (3 nadir and 1 backward) the data rate including image data, supplemental information and subsystem engineering data is 62 Mbps.

3. General aspects about DEM generation from satellite images

DEM of land surface provides significant information for many research activities and important data as the input of image processing and image analysis, such as image correction due to height of land surface (Ortho rectification), contour mapping, 3D images generation, disaster management (landslide, flood, etc.), monitoring land subsidence phenomenon and many others.

Digital elevation models are increasingly used for visual and mathematical analysis of topography, landscapes and landforms, as well as modeling of surface processes. A DEM offers the most common method for extracting vital topographic information and even enables the modeling of flow across topography, a controlling factor in distributed models of landform processes (Dietrich et al. 1993, Desmet & Govers 1995, Kirkby 1990). To accomplish this, the DEM must represent the terrain as accurately as possible, since the accuracy of the DEM determines the reliability of the geomorphometric analysis. Currently, the automatic generation of a DEM from remotely sensed data with sub-pixel accuracy is possible (Krzystek, 1995) (Kamp et al., 2003).

DEMs can be generated from stereo satellite data derived from electro-optic scanners such as ASTER. The ASTER sensor offers simultaneous along-track stereo-pairs, which eliminate variations caused by multi-date stereo data acquisition (Kamp et al., 2003).

A major advantages of the along-track mode of data acquisition (as compared to cross-track) is that the images forming the stereo pairs are acquired a few seconds (rather than days) apart under uniform environmental and lighting conditions, resulting in stereopairs of consistent quality that are well suited for DEM generation by automated stereocorrelation techniques (Akira, 2003, Fujisada, 1994).

Images generated from the nadir and aft telescopes yield had a B/H ratio of 0.6, which is close to ideal for generating DEMs by automated techniques for a variety of terrain conditions.

Digital photogrammetric techniques have been known for decades, but the possibility of using stereoscopic images from satellites for global digital elevation data production did not arise until the launch of the SPOT series in 1986. Today several satellites also offer the possibility for stereoscopic acquisition: SPOT (Priebbenow and Clerici, 1988), MOMS (Lanzl et. al., 1995), IRS, KOMSAT, AVNIR (Hashimoto, 2000), TERRA (Welch et al., 1998) and more recently, the high resolution pushbroom scanners IKONOS (September 1999), EROS-A1 (December 2000), QUICKBIRD-2 (October 2001), SPOT 5 (May 2002), and ORBVIEW-3 (June 2003) (tab. 1). Thus, some studies focus on constructing DEM from stereoscopic images by means of high resolution pushbroom scanners, IKONOS (Li et al., 2000, Toutin, 2001), EROS A1 (Chen and Teo, 2001.), SPOT 5 (Petrie, 2001); furthermore, it is assumed that the automatic generation of a DEM from remotely sensed data with a Z subpixel accuracy is possible (Krzystek, 1995) (Cuartero et al.).

Table 1. Satellite images used for DEM generation
(spatial resolution < 15 m)

Characteristics	Images						
	Quickbird	Ikonos	EROS-A1	SPOT-5/HRG	SPOT-5/HRS	IRS-PAN 1C/-1D	ASTER-VNIR
Ground resolution (m)	0.61 2.44	1 4	2.6	2.5, 5	10 (5)	5	15
Bands	PAN RGB, NIR	PAN RGB, NIR	PAN	PAN	PAN	PAN	G, R, NIR
Scene size (km x km)	16.5 x 16.5	11 x 11	12.5 x 12.5	60 x 60	120 x 60	70 x 70	60 x 60
Stereo acquisition	Along/across	Along/across	Along/across	Across	Along	Across	Along
Price for stereo scene	12240 $	Variable, min 4500 $	Variable, min 6200 $	Variable, min 9700 $	Only DEM	5000 $	55 $

The quality of digital elevation models (DEMs) elaborated from stereoscopic pairs is affected by the topography of the terrain and the data source (aerial photograms, digital satellite images), as well as other variables that depend on the data (aerial or spacial), on the algorithms used in the photogrammetric workstations, and on the data structure (triangulated irregular networks versus uniform regular grids).

A digital elevation model (DEM) can be extracted automatically from stereo satellite images. Numerous applications are based on DEM, and their validity directly depends on the quality of the original elevation data. High quality DEM are seldom available, even though photogrammetric technology, the most common to work with DEM has been around for a few years.

The accuracy of DEM elaborated from aerial stereoscopic pairs has been exhaustively analyzed but not all knowledge can be accepted in the spatial images case without a detailed analysis. Several factors distinguish both cases, e.g. the image spatial resolution, and the timing and geometric design of acquisition. These factors cause some common problems when using stereoscopic spatial images, e.g., the difficulty of identifying the Ground Control Points (GCP), or the existence of radiometric differences among the images due to acquisition at different dates that may make the stereo-matching process more difficult (Baltsavias and Stallmann, 1993). Nonetheless, it is clear that advantages such as wide coverage and good temporal resolution, give support to the general use of this data source.

Automation allows the construction of DEM with an almost randomly large point density. The selection of “very important points”, common in manual processing, is not applicable to automatic photogrammetric processes. The result often entails a very ‘hard’ DEM where a lot of redundant or unrelevant information can be removed. In literature review we could find no references to possible optimization strategies for this phase of the process. Accuracy estimation can be carried out by comparing the DEM data with a set of check points measured by high precision methods. The basic conditions for a correct work flow are: a) high accuracy of check points, and b) enough points to guarantee error control reliability.

Deriving DEM from stereoscopic satellite images is not new; however accuracy results and the method used to calculate error and reliability in DEM differ according to the literature revised. This variation may be due to the method used to estimate error in DEM as much in the number as in the source of check points used. The Algorithm Theoretical Basis Document, ATBD, for ASTER Digital Elevation Models (Lang & Welch, 1999) suggests that RMSE for Z values in ASTER DEM should be in the order of 10 to 50 m, but this is a too wide range to define the accuracy of a product (Cuartero et al.).

4. Material and study area

To produce digital terraine model it was used the AST_L1B_00309272003190545_10102003121021 ASTER image which was downloaded from the Internet. The image that was used has 14 bands, where bands *3n* and *3b* can be used for DEM generation (fig. 1). The image has a HDF-EOS (Hieratical Data Format) format and it is georeferenced in the Universal Transverse Mercator (UTM) projection sistem, on the WGS 84 ellipsoid. The satellite image that was used has the correction level 1B which means that it was processed to keep the original value in the image by appling the radiometric calibration and the geometric resampling coefficients.

The area that is studied is the 11 North area which has the minim altitude of 303,43 m and the maximum one of 2036,40 m.

The software that is used is ENVI 4.3 which has the power to produce the digital terraine model using the satelite images.

5. DEM generation

The geometric model being used is a rigorous one; it reflects the physical reality of the complete viewing geometry and corrects distortions that occur in the imaging process due to platform, sensor, earth, and cartographic projection conditions. After rigorous models (collinearity and coplanarity equations) are computed for the 3n and 3b images, a pair of quasi-epipolar images is generated from the images in order to retain elevation parallax in only one direction. An automated image-matching procedure is used to generate the DEM.

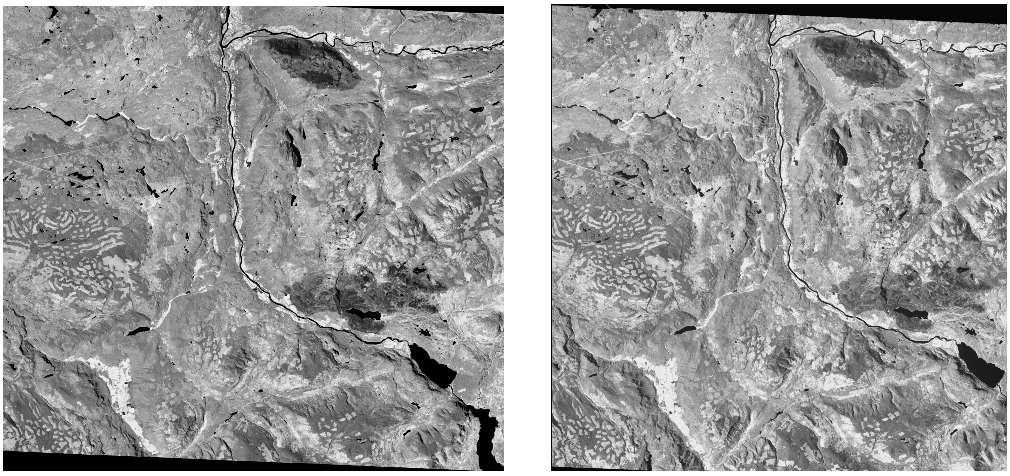

a. b.

Fig. 1. ASTER stereo images: a – left image, b – right image

Stage to achieve the DEM’s using as data sources the ASTER satelite images:

- *the introduction of the pair of images* and *the choosing of the type of model* that assumed the import of the image in ENVI 4.3 software and the choice of two bands (3n and 3b) for DEM generation;
- *the choosing of the type of model* assumes to establish the way in which the ground control points are used for DEM generation. If the ground control points are not used than it will be choise the relativ model that provides an accuracy of 10 m in the horizontal;
- he ground control points *can be defined in two ways*, *interactiv* or *importing* them into a folder that includes the coordinates of the points (the first 4 colums contain the coordinates of the image and the next 3 are coordinates expressed in the chosen projection). At this stage, for each point the image coordinates expressed in pixels in the two stereo images (the coordinates from the projection sistem that is chosen and their altitude) can be seen;

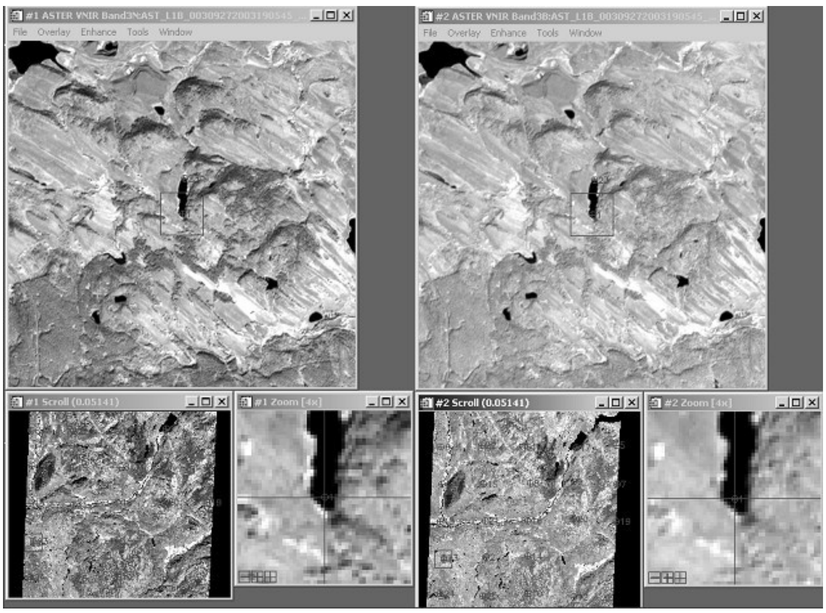

Fig. 2. Tie points generation

➢ *generating tie points* is a very important stage because according it the epipolar geometry of the image is obtained (Fig. 2). The tie points are diferent from the ground control points and have the role, just like in photogrammetry, to allow the matching of the satelile images. They can be obtained automatically, interactively or they can be imported from an out folder. In this case, tie points were obtained automatically and they number is 25. A correct choice of the number of tie points leads to the obtainance of a DEM which is much more appropiate to reality, providing a better matching between the two satelite images. Also important is the size of the window of analyse (search) which, in the case of images with a high spatial resolution, it has to be bigger. For this case it is established at 81;

➢ *the editation* and *examination of tie points* are done if they were generated automatically, like in this case. At this stage, which is also important, the aim is to eliminate *parallax on y* in order to obtain a high quality DEM. Also without eliminating the parallax on y, under some value, it cannot proceed to the next step. So, in this situation, initially the *y* parallax was of *40,7337 pixels* which has to be *decreased under 10 pixels* (tolerance established by the program). So tie points were edited on a list in descending order of positioning errors. The first point on the list that has the biggest positioning error is repositioned on both images and the new values that are obtained are updated on the point list (Fig. 3). The process repeated for the other points, in descending order of positioning errors until y parallax went down *under 10 pixels*, in this case being of *0,7337 pixels*. In some situations, after actualization the first point with the biggest positioning error, did not lead to the decrease of parallax y reason for which I went to these;

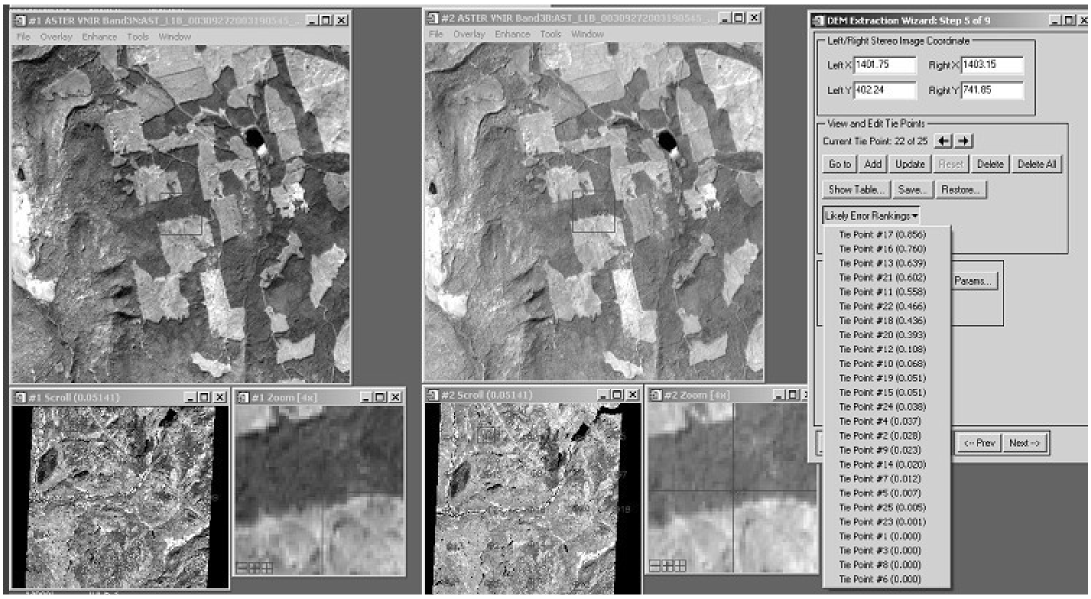

Fig. 3. Reduction of y parallax

➢ *collection of epipolar geometry* was based on two stereo images after the *y* parallax was reduced below 10 pixels. At this level, the stereo images are examined using the reducing epipolar coefficient with the value 1 in order to obtain a DEM with a resolution of 15 m. If the value of the reducing epipolar coefficient was 2, the DEM’s spatial resolution it would be of 30 m;

➢ *the configuration of the projection parameters* is based on information which formed the basis for the georeference of images and for the reduction epipolar factor chosen in the previous stage. In this sense, the projection system and datum were those of the input images and 15 m spatial resolution was chosen;

➢ *setting the parameters* for DEM generation I have to specify the correlation coefficient, the size of the window through which matching between the two images is made, the degree of land relief rendering and its details. Regarding the correlation coefficient it expresses the degree to which the two windows, the search and reference, match. As the coefficient is lower so the two windows are less correlated and the link is weaker. In general, the correlation coefficient with values between 0.65 and 0.85 is considered to be good. If there is used large reference and search windows than are also accepted values of a lower correlation coefficient. For the images studied the correlation coefficient was set at 0.95. In DEM generation an important role is achieving the pyramid image which is composed of several layers, each representing the same image but of a certain spatial resolution. In this sense, for restoring the macrorelief and the mesorelief it was chosen the maximum number;

➢ *DEM's extraction* was based on parameters defined in the previous stage (Fig. 4);

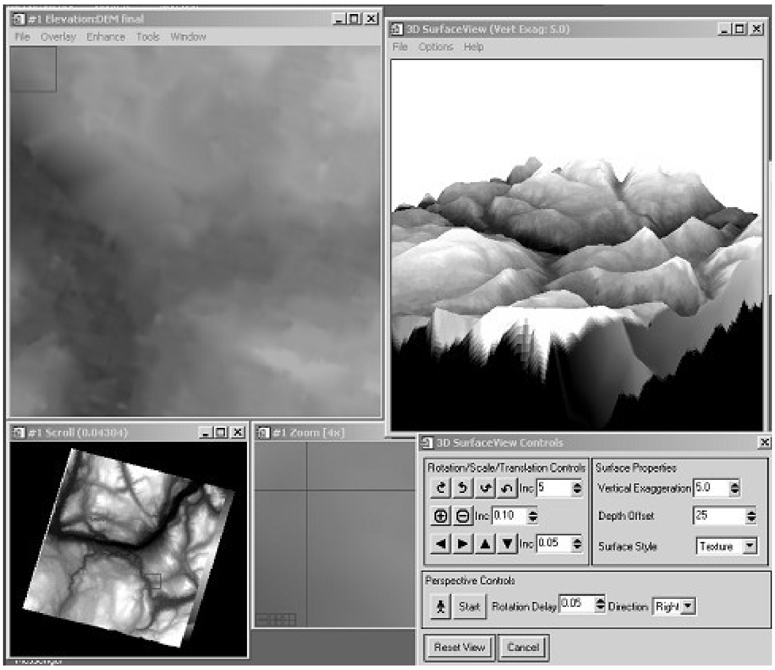

Fig. 4. Digital elevation model (2D and 3D)

➢ *processing DEM's* can be made for clear playback of relief using different filters (median, ironing, etc.) (Fig. 5).

6. Conclusions

ASTER images are alternative sources for extracting data to obtain DEM's, since these satellite records because are handy can be downloaded from the Internet.

Regarding the accuracy provided by DEM and its production methods by satellite images as ASTER, in the literature are a lot of research reports (Goncalves and Oliveira, 2004; Tsakiri-Strati et al, 2004; Pantelis et al, 2004; Ulrich et al, 2003). Some show that vertical accuracy of ASTER DEM is around *25 meters* and in areas devoid of vegetation it can increase vertical accuracy to *9-11 meters* (Goncalves and Oliveira, 2004; PCI Geo). In other studies (Ulrich et al, 2003) it is showed that ASTER's precision DEM is similar to maps made at *1:00000* and *1:50000* or even *1:25000*.

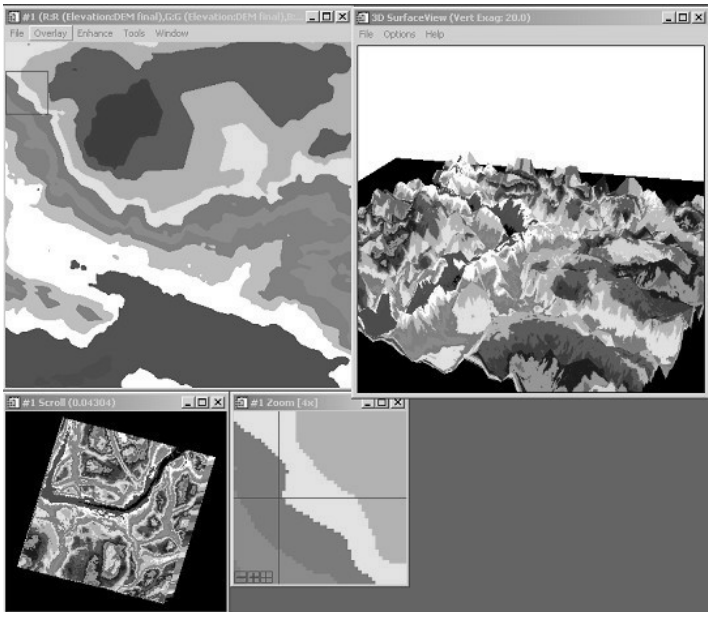

Fig. 5. Elevation classes (100 m each class) on DEM

Precision of data used to produce DEM may vary depending on the *types of surfaces* from where they are collected but the maximum horizontal error is up to *50 meters* and the maximum vertical error is, as mentioned above, between *9* and *25 meters*. It was found that ASTER images will produce a DEM's with a root mean square of less than a pixel in this case, thing that was also highlighted in other specialized works of foreign literature.

The number of control points is very important because it provides a basis for better or lower accuracy of the digital terrain model. It should also be considered the software that is used, each software having a specific algorithm. The algorithm cannot be changed during the completion of an ASTER DEM because it uses commercial software. Often, the software provides only a few parameters to get free selection by the operator. For identification, the operator must have experience in recognizing the image of the landform and that of land covers, given that TP's quality is essential to obtain a DEM of quality.

Although the digital model from this case was made only on control points automatically extracted from the two images, the absolute altitudes on ASTER DEM's have a good precision and allow the analysis of the mesorelief and macrorelief.

7. References

1. *Abrams, M., Hook, S., Ramachandran, B. - ASTER User Handbook. Version 2. Advanced Spaceborne Thermal Emission and Reflection Radiometer. Available at: http://asterweb.jpl.nasa.gov/content/03_data/04_Documents/aster_user_guide_v2.pdf; Accessed: 18.03.2010*
2. *Aniello, P. - Using Aster DEM to produce Ikonos orthophotos. ASPRS Annual Conference Proceedings, Alaska, May 2003;*
3. *Baipeng, LI., Qin, Y., Chunquan, C., Yanliangb, W., - The accuracy assessment experimentof ASTER 3d ortho product in Beijing area. The International Archives of the*

Photogrammetry, Remote Sensing and Spatial Information Sciences. Vol. XXXVII. Part B1. Beijing, 2008;

4. *Cuartero, A, Felicísimo, A.M., Ariza, F.J. - Accuracy of DEM genaration from TERRA-ASTER stereo data. Available at: http://www.isprs.org/proceedings/XXXV/congress/comm2/papers/191.pdf. Accessed: 18.03.2010*
5. *Hirano, A, Welch, R., Lang, H. - Mapping from ASTER stereo image data: DEM validation and accuracy assessment. ISPRS Journal of Photogrammetry & Remote Sensing 57, p. 356-370, 2003;*
6. *Kamp, U., Bolch, T., Olsenholler, J. – DEM generation from ASTER satellite data for geomorphometric analysis of Cerro Sillajhuay, Chile/Bolivia. ASPRS 2333 Annual Conference Proceedings May 2003, Anchorage. Alaska, 2003;*
7. *Lee, J.D., Han, S.H., Lee, S.S., Park, J.S. - Correcting DEM extracted from aster stereo images by combining cartographic DEM. The International Archives of the Photogrammetry, Remote Sensing and Spatial Information Sciences. Vol. XXXVII. Part B1. Beijing, 2008;*
8. ***** Tutorial ENVI;*
9. ***** http://webmap.em.gov.bc.ca/mapplace/minpot/aster.asp*